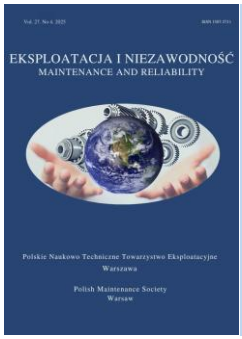

Eksploatacja i Niezawodnosc – Maintenance and Reliability

Volume 27 (2025), Issue 4

journal homepage: http://www.ein.org.pl

Article citation info:
Ezhil Jenekkha G. B, Marsaline Beno M, Jebarani Evangeline S, Sridharan S, Artificial Intelligence-Based Soft-Charging Dual Boost Control: PSO-Tuned Reactive Power Compensation for Reliability and Maintenance in Medium Voltage Unbalanced Grid Networks, Eksploatacja i Niezawodnosc – Maintenance and Reliability 2025: 27(4) http://doi.org/10.17531/ein/203804

Artificial Intelligence-Based Soft-Charging Dual Boost Control: PSO-Tuned Reactive Power Compensation for Reliability and Maintenance in Medium Voltage Unbalanced Grid Networks

Indexed by: Web of Science Group

Ezhil Jenekkha G. B[a], Marsaline Beno M[b,*], Jebarani Evangeline S[c], Sridharan S[d]

[a] Electrical and Electronics Engineering, M.E.T. Engineering College, Nagercoil, Tamilnadu, India
[b] Electrical and Electronics Engineering, St. Xavier's Catholic College of Engineering, Nagercoil, Tamilnadu, India
[c] Electrical and Electronics Engineering, SNS College of Engineering, Coimbatore, Tamilnadu, India
[d] Electrical and Electronics Engineering, St. Joseph's College of Engineering, Chennai, Tamilnadu, India

Highlights

- Ensures stable electricity transfer to the grid.
- Enhances DC-link voltage regulation and grid stability.
- Improves system reliability under three-phase disturbances.
- Enhances power transfer efficiency and grid-side regulation.

Abstract

The Proposed Artificial Intelligence (AI) based Soft Charging Double Boost-Modified Dual Controller (SCDB-MDC) is designed with current controllers which are intended to regulate the flow of electricity between the grid and Distributed Generator (DG) units. To regulate the voltage of the DC-link in the Soft Charging-MDC unit, which should be an additional responsibility of injecting electricity into the grid network, a fuzzy-tuned AI controller based on Particle Swarm Optimization (PSO) is presented. Magnitudes of line currents would reach higher values than the nominal values during unbalanced which is the main drawback of the conventional Dual Vector Current Control (DVCC). MDC is proposed with a line current limiter for parallel inverters. Grid currents would reach higher values during such disturbances are prevented by modifying current reference calculation in the proposed controller. This work demonstrates the effectiveness of SCDB-MDC in maintaining operational reliability and facilitating robust power management in medium-voltage unbalanced grid networks.

Keywords
single source inverter, distributed generator, double boosting soft charging MDC unit, particle swarm optimization, unbalanced condition.

1. Introduction

A novel Single Source Inverter (SSI) with reduce aspect count topology is supplied within the research paper. furthermore, it makes use of switching capacitor period for the operation and it boosts the voltage by twice the input voltage [1]. STATCOM under investigation is tuned using the Water Cycle Algorithm (WCA), Particle Swarm Optimization (PSO), and a hybrid algorithm of both WCA and PSO [2]. The problem caused by intermittent energy sources that are connected to a balanced/unbalanced distribution system using a superconducting magnetic energy storage (SMES) system by mitigating the voltage and frequency fluctuations during wind gusts [3]. The development of the structure of a fast and flexible

(*) Corresponding author.
E-mail addresses: Ezhil Jenekkha G. B (ORCID: 0000-0003-4246-6442) ezhiljenekkha@gmail.com, Marsaline Beno M (ORCID: 0000-0002-8189-5613) beno@sxcce.edu.in, Jebarani Evangeline S (ORCID: 0000-0002-2762-285X) reachjebarani@gmail.com, Sridharan S (ORCID: 0000-0002-5300-8319) sridharans@stjosephs.ac.in

data collecting system based on the proposed approach to measure power quality indicators in three-phase medium-voltage distribution grids with an example of a Mikhailovsky mining and processing plant [4]. Superconducting magnetic energy storage (SMES) systems are used to mitigate voltage and frequency changes during wind gusts, which is an issue created by intermittent energy sources connected to a balanced/unbalanced distribution system [5].

Improved voltage and power stability of isolated microgrids is mostly achieved through the use of robustly-controlled energy storage systems. Energy storage system integration, particularly superconducting magnetic energy storage, or "SMES," with DC-bus microgrids was the subject of relatively few studies [6]. One of the most noteworthy ways to lessen dependency on fossil fuels and, consequently, the effects of pollution is to use renewable energy sources (RESs). Technologies like solar photovoltaics (PV), wind power generation (WPG), or both are employed to address various problems in the electric power grid [7]. Variability in system voltage and power is increased by modern power systems' improved access to renewable sources.

The intermittent nature of renewable energy sources (RESs) and their reliance on solar irradiance and wind speed, respectively, are also major challenges in their use [8]. Using a Photovoltaic (PV)-based Dynamic Voltage Restorer (PV-DVR), a new method for improving power quality has been introduced. The suggested effort is intended to solve flicker, harmonics, and voltage fluctuations in medium or low voltage micro-grid systems [9]. This study offers optimization and techno-economic feasibility analyses of suggested hybrid renewable systems, as well as their overall cost impact in stand-alone and grid-connected modes of operation, for the diesel generators that are connected to the University of Debre Markos' electrical distribution network with hybrid renewable energy sources [10].

Because of their superior output voltage ranges, MLIs have lower output voltage hole harmonic distortion (THD) than two-level inverters. Its compact output filter out size, low electromagnetic interference, and low device stress voltage have made them very popular [11]. Among various power quality issues in a micro-grid, a severe issue that reduces the performance of the converter is un balance in the voltage in a three-phase system. Unbalance in voltage deteriorates the performance of the micro-grid by inducing twice the frequency ripples [12]. When Distributed Generators (DG) connected during unbalance load serious issues are created and it's expected to be disconnected during voltage disturbances to avoid stress on the grid. [13]. A control strategy is developed such that DGs are connected during the disturbances and they can support the grid in such situations provided there is no power flow from DGs to grid [14].

Yameen et al. [15] Static synchronous compensator (STATCOM) tuning methods like as fuzzy logic, ant colony, and evolutionary algorithms have been used in the past by researchers to improve microgrid stability in fault scenarios. Hasheminasab et al. [16] With the advent of Distributed Energy Resources (DERs), the energy landscape is fundamentally changing to become more robust and ecologically benign. Inverter-based DER integration presents difficulties, nevertheless, especially with regard to grid instability and system inertia. Hattabi et al. [17] Different metaheuristic algorithms are tested and compared using various fitness functions employing the latter System Coordinating Council (WSCC), the New England 10 machine 39-bus power system, and the single machine infinite bus system (SMIB). El Sayed et al. [18] A double line to the ground fault that applies to this system is one example of an asymmetric fault that causes it, as are three-phase symmetric faults.

Yegon et al. [19] the primary and significant issues with the electricity infrastructure. Three-phase symmetric faults & asymmetric faults, such the double line to ground fault that applies to this system, are the causes of it. Mondal et al. [20] Comparing the findings to traditional particle swarm optimization, it is possible to see that the frequency nadir is improved by 48.96% while the rate of frequency change is significantly reduced. Ravi et al. [21] Despite distributed generation's (DG) many advantages, including its environmentally friendly nature and consistent energy supply, connecting DG with the grid presents a number of difficulties.

Iweh et al. [22] Primarily focused on the classification of distributed generation (DG), the difficulties in integrating DG to the grid, the useful choices for doing so, the lessons discovered from some nations that had successfully integrated DG to the grid, the causes that drove the expansion of DGs, and

the benefits of DG to grid integration. Alharbi [23] Unbalanced voltage at the common coupling point is considered. This point will have an oscillating power which is eliminated by control strategies for grid-connected inverter. Alathamneh et al. [24] This paper suggests utilizing a proportional-resonance controller to regulate the real and reactive power of a three-phase grid-connected inverter in both directions when the grid is not balanced. Joshi et al. [25] outlines a novel algorithm in natural coordinates for managing grid-connected photovoltaic (PV) systems using load correction features when grid voltages are distorted and out of balance. Nikolaev et al. [26] The current state of power system stability research by offering a thorough analysis of how PV generation affects small-signal stability and the latest developments in POD control using PV inverters.

Tiwari et al. [27] A construction, operation, modulation technique, capacitor values, and circuit losses are described to illustrate the proper operation of the proposed topology. Hata et al. [28] By lowering the inductor current in relation to the load current, dual-path hybrid DC-DC converters can increase efficiency. However, when the switching frequency is constrained, the presence of spike currents from the switched capacitor makes it more difficult to reduce passive components. Abbasi et al. [29] suggests an isolation-based plan that makes use of the switched capacitor multilevel inverter's flyback converter. Additionally, with fewer power switches, the total design provides step-up AC voltage across the load from a single DC supply. Anand et al. [30] To reduce the charging current ripples across the capacitors, quasi-soft charging is used in conjunction with a thorough investigation of capacitor selection and sizing.

The main contributions of this paper are: The primary contribution is to improve the steady state and transient performance indices by designing the controller's dynamic gain parameters to manage system uncertainties. Enhancing the computational cost and convergence for ill-conditioned systems operating under numerous working points is a significant contribution in this subject. Improved transient response and less strain on power components are two benefits of using a current-fed converter.

2. Block Diagram of Proposed SSI Double Boosting MDC Unit

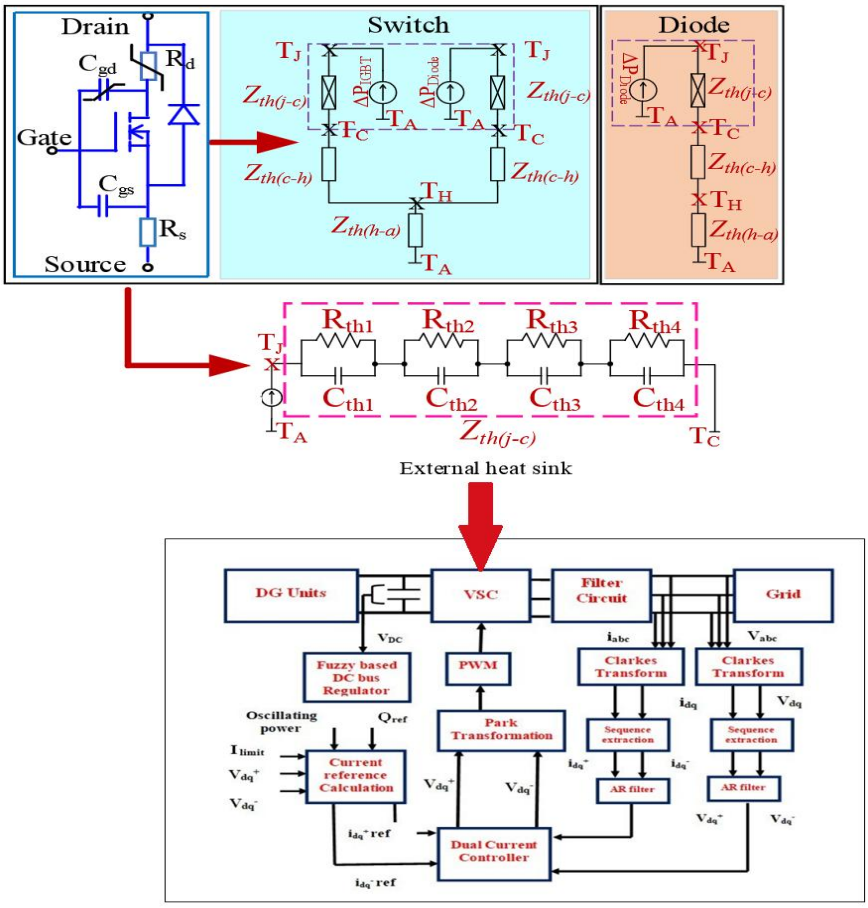

Fig. 1. Block diagram of proposed SSI Double boosting MDC unit.

Any disturbance that occurs in the grid would lead the entire system into unstable conditions. It is also not good to disconnect the DGs at the time of the disturbances. DGs have to be connected for compensation without providing any oscillating power during such disturbances.

The proposed controller's overall block diagram is displayed in Fig. 1. Under such unbalanced voltage conditions, the controller's primary responsibility is to regulate the power flow from DG to the grid while also providing voltage compensation. Anti-Resonant Filter (ARF), sequence extraction, and voltage source converter design are outside the purview of this study as they have already been covered in [5]. This paper mainly concentrates on the reference current generation and PSO based fuzzy tuned AI parameters for the control of DG units.

3. Description of Real and Reactive Power for Current Reference Calculation

The current reference to be given as the input to MDC can be calculated using the complex power. The complex power of the grid in $\alpha\beta$ frame is given by Equation (1).

$$S = v_{\alpha\beta}\, i_{\alpha\beta} = p(t) + jq(t) \tag{1}$$

Similarly, the complex power of the grid in dq frame is given by the Equation (2).

$$S = \left(v^{p}{}_{dq} e^{j\omega t} v^{n}{}_{dq} e^{-j\omega t}\right)\left(i^{p}{}_{dq} e^{j\omega t} i^{n}{}_{dq} e^{-j\omega t}\right) = p(t) + jq(t) \tag{2}$$

Reactive power q(t) and active power p(t) are measured instantly utilizing

$$p(t) = P_{avg} + P_{cos\,2}.cos(2\omega t) + P_{sin\,2}.sin(2\omega t) \tag{3}$$

$$q(t) = Q_{avg} + Q_{cos\,2}.cos(2\omega t) + Q_{sin\,2}.sin(2\omega t) \tag{4}$$

The terms P_{avg} and Q_{avg} denote average active and reactive power respectively. Terms Sin(2wt) and Cos(2wt) represents the oscillating part of the power due to unbalance. The above factors are related to voltages and currents as in the following equations.

$$P_{avg} = (v_d{}^{p} i_d{}^{p} + v_q{}^{p} i_q{}^{p} + v_d{}^{n} i_d{}^{n} + v_q{}^{n} i_q{}^{n}) \tag{5}$$

$$P_{cos\,2} = (v_d{}^{p} i_d{}^{n} + v_q{}^{p} i_q{}^{n} + v_d{}^{n} i_d{}^{p} + v_q{}^{n} i_q{}^{p}) \tag{6}$$

$$P_{sin\,2} = (v_q{}^{n} i_q{}^{p} - v_d{}^{n} i_q{}^{p} - v_q{}^{p} i_d{}^{n} + v_d{}^{p} i_q{}^{n}) \tag{7}$$

$$Q_{avg} = (v_q{}^{p} i_d{}^{p} - v_d{}^{p} i_q{}^{p} + v_q{}^{n} i_d{}^{n} - v_d{}^{n} i_q{}^{n}) \tag{8}$$

$$Q_{cos\,2} = (v_q{}^{p} i_d{}^{n} - v_d{}^{p} i_q{}^{n} + v_q{}^{n} i_d{}^{p} - v_d{}^{n} i_q{}^{p}) \tag{9}$$

$$Q_{sin\,2} = (v_d{}^{p} i_d{}^{n} + v_q{}^{p} i_q{}^{n} - v_d{}^{n} i_d{}^{p} - v_q{}^{n} i_q{}^{p}) \tag{10}$$

The matrix representation of equations (5)–(10) is as follows:

$$\begin{bmatrix} P_{avg} \\ Q_{avg} \\ P_{sin\,2} \\ P_{cos\,2} \end{bmatrix} = \begin{bmatrix} v_d{}^{p} & v_q{}^{p} & v_d{}^{n} & v_q{}^{n} \\ v_q{}^{n} & -v_d{}^{p} & v_q{}^{n} & -v_d{}^{n} \\ v_q{}^{n} & -v_d{}^{n} & -v_q{}^{n} & v_d{}^{n} \\ v_d{}^{n} & v_q{}^{n} & v_d{}^{p} & v_q{}^{p} \end{bmatrix} \begin{bmatrix} i_d{}^{p} \\ i_q{}^{p} \\ i_d{}^{n} \\ i_q{}^{n} \end{bmatrix} \tag{11}$$

The $V_d{}^{+}, V_q{}^{+}, V_d{}^{-}, V_q{}^{-}$ denotes the positive and negative dq sequence components of the voltages, whereas idp, iqp, idn, iqn stand for the current components. In order to avoid using the $6X6$ invertible matrix, oscillating reactive power is not used into the current reference computation. As a result, the system would experience uncontrolled oscillating reactive power.

3.1. Current Reference Calculation for Modified Dual Controller

The calculation of current reference is a vital feature for controlling the negative current on the power system and to provide a better grid connected renewable energy system even under the grid disturbances like voltage unbalance. The current reference is calculated using Equation (11). The constant dc-link voltage across the capacitor is the expected constraint for the converters. The reference current calculated has to suppress the current-error vector. The grid current effects are considered when the reference current is calculated for the controller.

$$\begin{bmatrix} I^{2}{}_{grid} \\ Q_{avg} \\ P_{sin\,2} \\ P_{cos\,2} \end{bmatrix} = \begin{bmatrix} I^{2}{}_{Limit} \\ Q_{ref} \\ P_{sin\,2} \\ P_{cos\,2} \end{bmatrix} = \begin{bmatrix} i_d{}^{p} & i_q{}^{p} & i_d{}^{n} & i_q{}^{n} \\ v_q{}^{n} & -v_d{}^{p} & v_q{}^{n} & -v_d{}^{n} \\ v_q{}^{n} & -v_d{}^{n} & -v_q{}^{n} & v_d{}^{n} \\ v_d{}^{n} & v_q{}^{n} & v_d{}^{p} & v_q{}^{p} \end{bmatrix} X \begin{bmatrix} i_d{}^{p} \\ i_q{}^{p} \\ i_d{}^{n} \\ i_q{}^{n} \end{bmatrix} \tag{12}$$

$$\begin{bmatrix} i_d{}^{p}{}_{ref} \\ i_q{}^{p}{}_{ref} \\ i_d{}^{n}{}_{ref} \\ i_q{}^{p}{}_{ref} \end{bmatrix} = \begin{bmatrix} i_d{}^{p} & i_q{}^{p} & i_d{}^{n} & i_q{}^{n} \\ v_q{}^{n} & -v_d{}^{p} & v_q{}^{n} & -v_d{}^{n} \\ v_q{}^{n} & -v_d{}^{n} & -v_q{}^{n} & v_d{}^{n} \\ v_d{}^{n} & v_q{}^{n} & v_d{}^{p} & v_q{}^{p} \end{bmatrix}^{-1} X \begin{bmatrix} I^{2}{}_{Limit} \\ Q_{ref} \\ -\Delta P_{sin\,2} \\ -\Delta P_{cos\,2} \end{bmatrix} \tag{13}$$

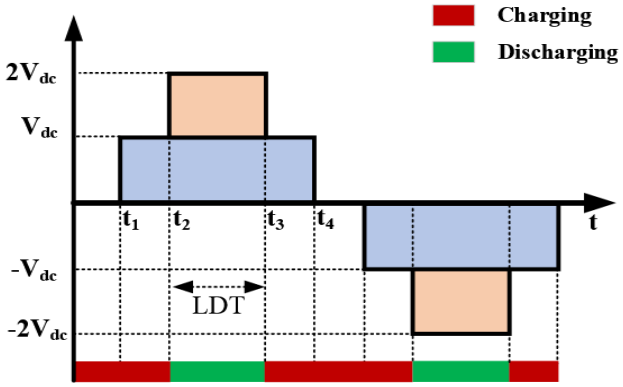

Fig. 2. Proposed SC-MDC strategy with Charging and discharging unit.

Figure 2, displays the block diagram for the suggested

approach. In a conventional DVCC $\mathbf{P_{avg}} = \mathbf{P_{ref}}$ which aims at the desired power flow from the DG units. But in the proposed controller this is replaced by $\mathbf{I^2_{limit}} = \mathbf{I^2_{grid}}$. Active power is replaced with current term because the active power is generally deduced from the grid voltages and current. And by the calculation of the actual current, the required active power can be estimated. The proposed algorithm calculates reference current values using current limit, reactive power reference, and by demanding the grid to supply the required oscillating active power $\mathbf{P_{sin2}} = -\Delta\mathbf{P_{sin2}}$, $\mathbf{P_{cos2}} = -\Delta\mathbf{P_{cos2}}$. As a result, the filter and dc-link do not experience fluctuating active power flows. The decrease in grid voltages and constrained currents results in a decrease in the power delivered by the DG units. Reactive power oscillations are not eliminated however using this strategy, since those terms are not included in the reference current calculation. The impact of negative sequence components during grid disturbances is reduced.

3.2. PSO Based Fuzzy-Ai Controller Design

The algorithm for power flow control establishes the power level that should be sent between distributed generation units and the grid. Better compensation for voltage imbalance is provided by the proposed SCDB-MDC technique, particularly in instances of significant grid outages. The results show that the SCDB-MDC method increases the unbalanced voltage compensation to 0.35%, although prior AI-based and PSO-tuned controllers (as shown in references such as Ren et al., 2018 [31] and Bimbhra & Garg, 2014 [33]) achieve this ability in the range of 0.25%–0.30%. This high compensation % shows that the proposed strategy works to keep the grid voltage steady in imbalanced situations, which guarantees improved performance during faults or abrupt changes in load. Two crucial elements of the control technique during voltage maintenance are dc-link voltage maintenance and dc-link power regulation. deploying a fuzzy-AI controller based on PSO. Voltage imbalance, such as voltage sag, causes the converters that convert electricity to undergo a decrease in voltage magnitude. Grid power would decrease as a result, and current should be raised to maintain an even grid power level. This raises the dc-link voltage and restricts the amount of electricity that DGs may transmit to the grid during voltage sag. In comparison to other approaches to optimization, the fuzzy-tuned AI controller with PSO was selected for its effectiveness, real-time adaptability, and higher optimization skills in managing the complex structure of grid disturbances.

The differential equations for the dc connection are as follows:

$$P_{DG} = P_1 + P_2 \tag{14}$$

$$P_L = P_{DG} + P_G \tag{15}$$

$$Q_L = Q_{DG} + Q_G \tag{16}$$

where P_1, P_2 are the respective powers of DG_1 andDG_2.P_G, P_L are the respective grid and load power. Q_G, Q_L represent corresponding reactive powers. The following equation gives the dc link power balance relation.

$$C_{dc}V_{dc}\frac{dv_{dc}}{dt} = P_1 + P_2 - P_G \tag{17}$$

As per the above equation, for maintaining constant dc voltage across dc-link capacitor, power balance in the capacitor has to be maintained. Any imbalance on the grid side would alter the grid power, which would disrupt the dc-link voltage. The energy equation provided determines how much power must be absorbed in order to maintain a power balance in a dc link,

$$E_{dc} = \left(\frac{1}{2}\right) C_{dc}v^2{}_{dc} \tag{18}$$

The following formula is used to construct a power flow control strategy that establishes how much energy should be stored in a battery for a parallel inverter during voltage unbalance. The controller is provided with two inputs: error and error change rate. The discrepancy between the reference energy and the actual stored energy provides the controller with the error input.

$$e = E_{dc-ref} - E_{dc} \tag{19}$$

Where, $E_{dc\text{-}ref}$ is dc link reference energy and E_{dc} is the energy of dc link voltage. The rate of change of error input is given by,

$$\Delta e(n) = e(n) - e(n-1) \tag{20}$$

Error and rate of change of error are the inputs for a PSO based fuzzy AI tuned controller.

Figure 3 illustrates the reactive power production employing a fuzzy-AI controller method based on PSO and the proposed reactive power compensation of an imbalanced grid with lower THD. The following steps are the original formulations that, in accordance with the idea, can increase its efficiency with the particle changes:

- The initial velocity is developed and assigned to the starting particles in DG unit values at the beginning of the particles swarm algorithm.
- The optimal function and location value are determined by evaluating the objective function in each particle location. In order to identify their own optimal places in relation to their neighbors, the particles select new velocities based on the existing velocity.
- A collection of random particles is initialized in PSO, and subsequent generations are updated to optimize the group. In each iteration, the fuzzy-AI controller is used to adjust the PSO parameters, and each particle is updated with the two best values.
- Fig. 4 and Table 1 illustrate how the method iteratively updates the neighbor and moves the particle's locations and velocities until it meets a stopping threshold.

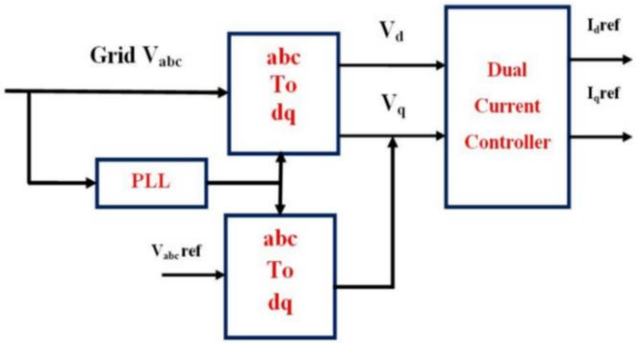

Fig. 3. Fuzzy AI based voltage controller.

We have created two PSO algorithms with different neighborhood sizes. The first one is G_{best} PSO, where the neighborhood of each particulate is determined by the velocity (v) equation for the entire swarm. The particle swarm with the optimal optimizer value is known as P_{best} . Local best, represented by L_{best} , is another "$best$" value that has been monitored thus far, where each particle's smaller neighborhood is specified as being in the population.

$$V_{ij} = V_{ij}(t) + C_1R_1(t)\left[Y_{ij}(t) - X_{ij}(t)\right] + C_2R_2j(t)$$
$$[\hat{Y}_j(t)\text{-}X_{ij}(t)] \quad (21)$$

Where,

V_{ij} (t)- The particle's speed at one moment (t),

i- Dimension,

j-1, 2,…….N,

X_{ij}(t)- Particle position at a given time (t),

C_1, C_2 - Positive acceleration constants.

R_1, R_2 - Random numbers between 0 and 1.

The best position that particle I has visited is its personal best position, yi, since the first step and the subsequent time step $(t+1)$ are computed as,

$$X(t+1) = X(t) + V(t+1) \quad (22)$$

The velocities of the particles are divided in the parts, (1) Previous velocity, (2) Cognition component, and (3) Social component. Cognitive and social component contributions are weighted according to their respective stochastic amounts, C_1R_1 or C_2R_2. When a particle chooses some of the population as its topological neighbors, the best value is a local best that enters the search space. Following the discovery of the two best values, the particles' locations and velocity are updated in the equations (21) and (22) where each particle can broaden the search criteria based on the current best value.

Table. 1 Control parameters.

Parameters	**Value**
weight of inertia, w	09 ~0.4
Random variables [R_1, R_2]	[0,1]
No. of particles	50
Max. criteria	100 iterations
Cognitive factor, C_1	0.03
Social factor, C_2	0.90
No. of population	50
Best MI (Ma)	0.51

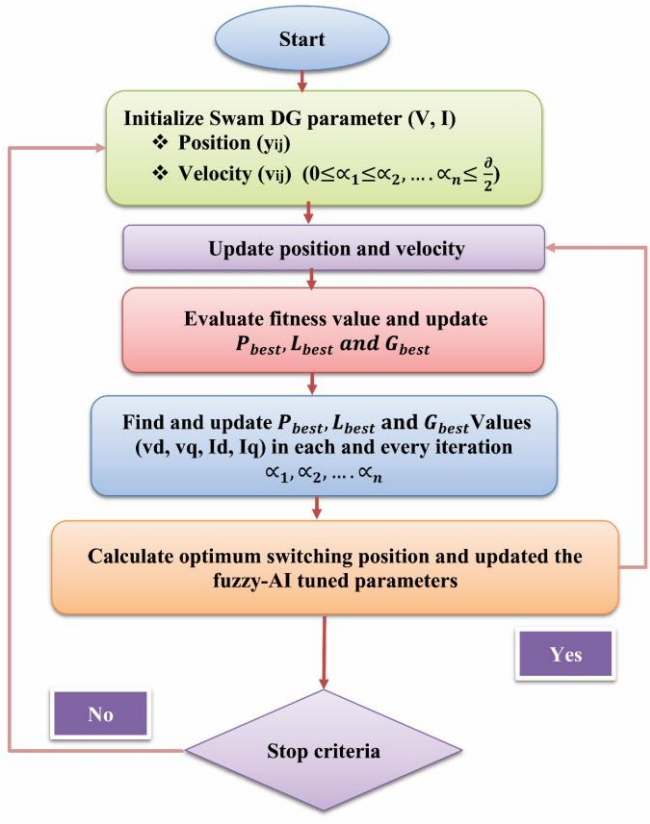

Fig. 4. PSO based Fuzzy-AI tuned parameters.

3.3. Voltage Regulation Capability

The DG unit uses UC provide to voltage support, if voltage regulation capability is included with based on system controller. The main task is to inject required power and the additional task is to regulate the voltage. To prevent the inverter from overloading, the current controller limits the converter current when it is out of balance. Therefore, the reactive power needed for compensation would not be provided by DGs. Reactive power consumption is lowered or perhaps eliminated when the DG units are operating at full capacity. Issues occur when the load is reduced or when there is a high generation condition. The active power determines how much reactive power can be used at its highest level. It can be expressed as,

$$Q_{DG\,lim\,it} = \sqrt{(V_{DG\,lim\,it} I_{DG\,lim\,it})^2 - (P^2{}_{DG})} \qquad (23)$$

Where, QDG limit is the maximum reactive power, $V_{DGlimit}$ is the maximum DG voltage, $I_{DGlimit}$ is the maximum DG current, P_{DG} is the maximum DG power. Voltage regulation at point of common coupling is performed by injecting reactive power into the grid.

4. Simulation and Experimental Results

The simulation's parameters are shown in Table 2. In this study, the simulation and experimental findings are compared, and the simulation parameters are selected in accordance with the reference [14]. Fig. 5(a), depicts an experimental arrangement for soft shifting MDC units. The simulation and lab testing parameters were same in order to further confirm the efficacy of the suggested hardware configuration with the FPGA (Xilinx-5) controller, which is displayed in Fig. 24. FPGA controller is used to comparing the simulation results that are obtained by using an MDC based fuzzy AI controller. The unbalanced grid voltage is simulated using a programmable voltage source. The power stage is consisting of a dual parallel inverter with DC-link voltage provided by DC power supply. The Xilinx-5 platform is compiled into VHDA- code before programmed onto the FPGA chip. The PWM controller triggers pulses based on the FPGA controller. Therefore, FPGA assists with fuzzy logical rules using AI technique. Unbalance is created at different time intervals using a programmable voltage source, and LC combination is used as a filter circuit.

A digital storage oscilloscope (DSO) can be used to examine the experimental findings, which include grid voltage, grid current, MDC link voltage, active power, and reactive power, in cases where a controller has been set up to govern control parameters and reference values. The grid voltage during an imbalance caused by a voltage source is known as Channel 1. The current plot is displayed in Channel 2 for the duration of the input variations. The voltage across the DC-link is displayed in Channel 3 and is kept constant. Measured in channel-4, the injected reactive power used to maintain the imbalance can be compared to the simulated waveform displayed in Fig. 21. Comparing the proposed three-phase grid voltage to the literature evaluation for current techniques, this paper suggests an imbalanced degree of improvement in voltage control and efficiency level in Table 3.

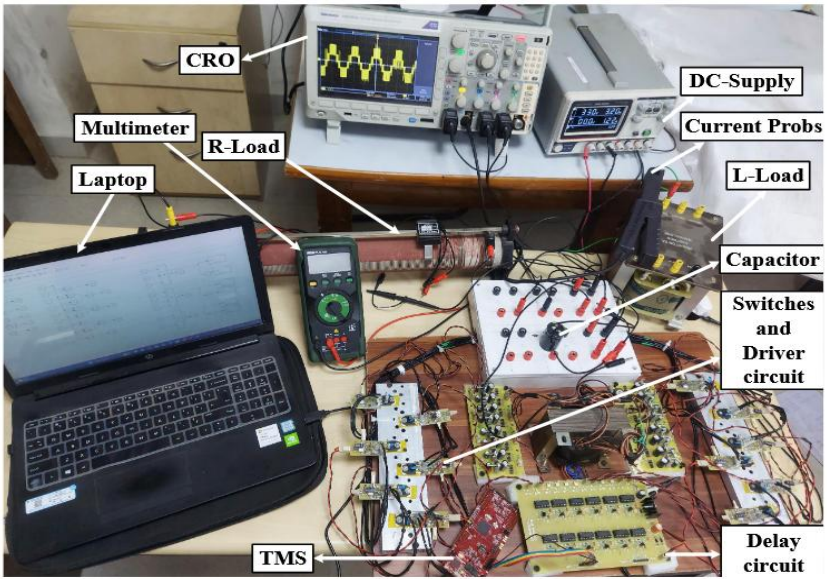

Fig. 5. (a) Proposed Soft Changing Double Boost MDC Unit.

4.1. Case 1: Operation Under Normal Conditions

During normal conditions fixed amount of power is scheduled to be supplied by the grid and the remaining to be delivered by the DGs. Proposed grid DG's. The controller is designed to supply scheduled power from the grid and the remaining power by DGs. The parallel unit's active and reactive powers, along with the corresponding reference powers, are displayed in Fig. 5(b) and Fig. 6. With a very small overshoot control strategy tracks the reference active power. It is seen that when the reference power changes, DG power also varied during transient for maintaining dc-link power.

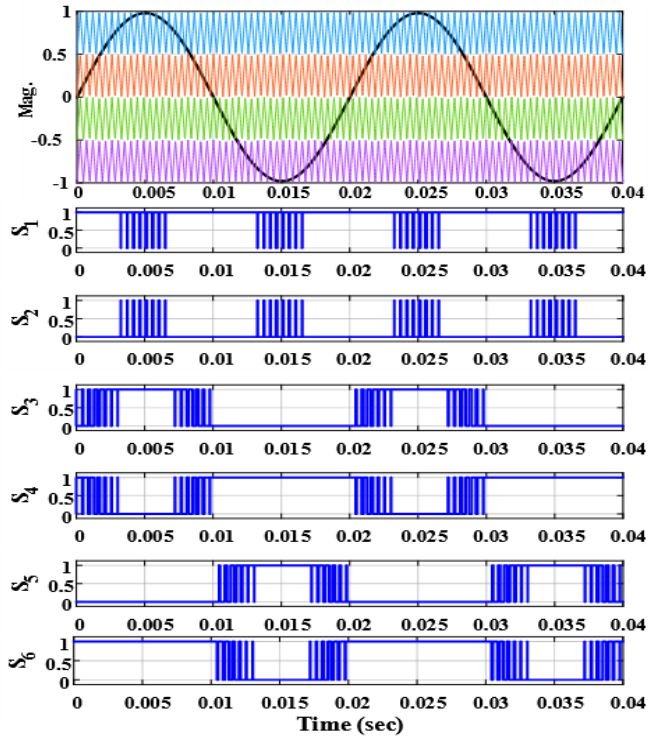

Fig. 5. (b) Active power delivered to the grid with proposed methods.

Table 2. System Modeling Parameters.

Parameters	Values
Grid voltage	400 V
Grid Frequency	50Hz
R_1 (Resistance)	1.6mΩ
L_1 (Inductance)	0.52mH
R_2	0.6 mΩ
L_2	0. 2mH
R_g (Grid Resistance)	0.15Ω
L_g (Grid Inductance)	6.15mH
DC link capacitance	550 µF
MATLAB integrated version	2023a

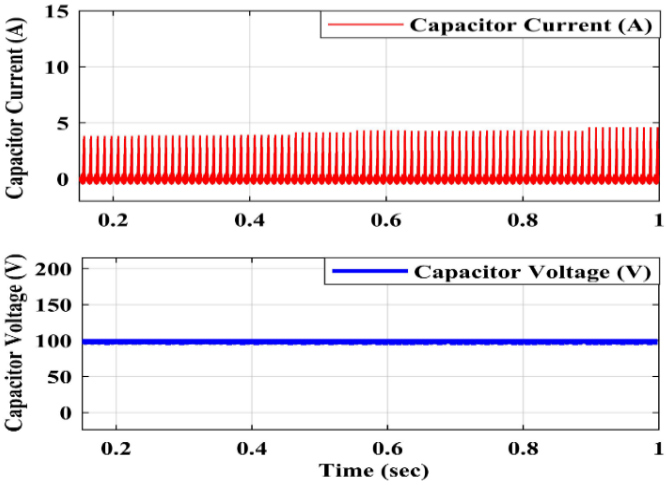

Fig. 6. Reactive power delivered to the grid with soft switching charging boost-MDC unit.

4.2. Case 2: Power Flow Control During Under Unbalanced Conditions

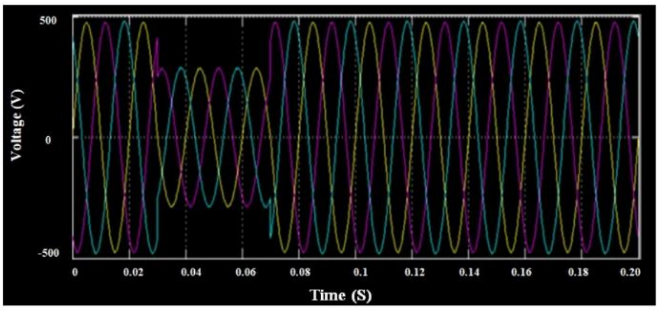

Fig. 7. Grid voltages due to sag.

The proposed controller is tested for unbalance grid conditions. A 60% voltage drop is used to generate the voltage sag, which lasts for 0.03 to 0.07 seconds. In Fig. 7, the grid voltage is displayed. In Fig. 8, the grid currents are displayed. It is evident that the current controller's existence makes the current values nearly equal to the typical current. Current controllers react more quickly to track the changing references and follow a pure sinusoidal waveform following voltage sag. DG1 and DG2's instantaneous active power is displayed in Fig. 8. The curves overlap because the power of DG1 & DG2 is equal.

Figure 8, shows that during sag, the amount of power that DGs inject into the grid decreases. During the 0.03 to 0.07 second interval, there are some oscillations on active power because of the voltage drop. The grid must deliver these fluctuating active powers. Thus, the filter and dc-link do not experience oscillatory active power flows. Fig. 9, illustrates the reactive power delivered by DG1 and DG2.

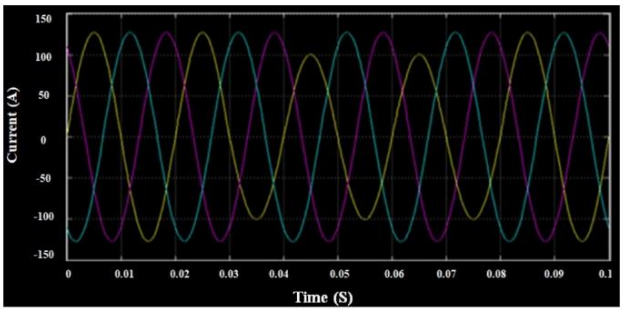

Fig. 8. Grid currents due to sag.

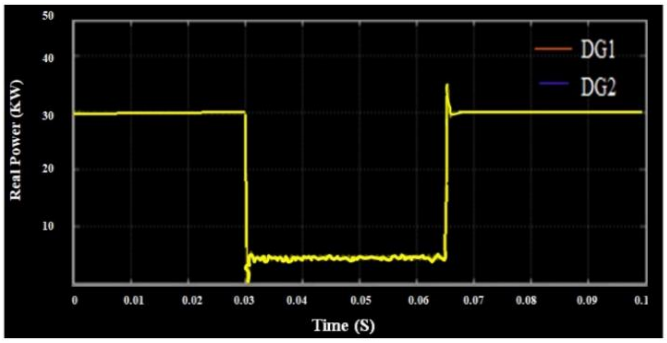

Fig. 9. Active power by DG1 and DG2.

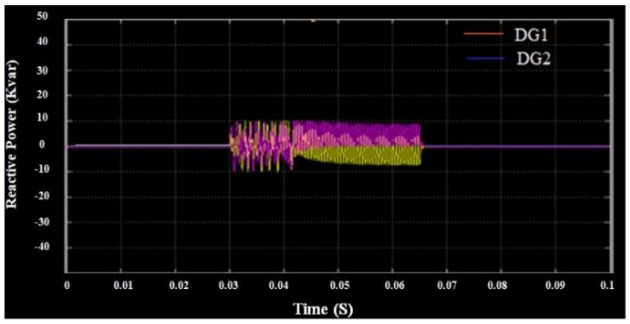

Fig. 10. Reactive power by DG1 and DG2.

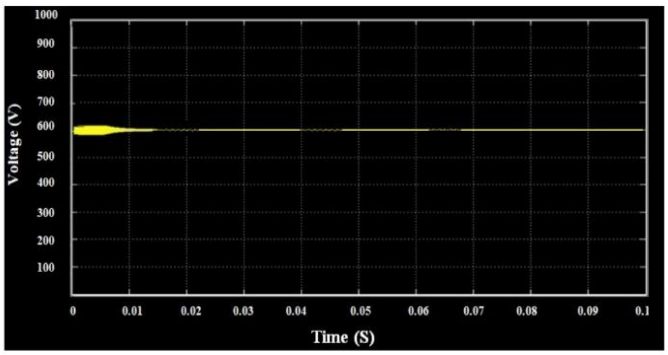

Fig. 11. DC link voltage.

It is evident from Fig. 10, that there are significant oscillations when sag occurs. It is because the controller does not respond to reactive power. Fig. 11, depicts the voltage across the direct current link. During sag, the dc-link voltage increases slightly, but not by more than 5% of its typical value. In these grid disruption scenarios, a fuzzy-AI controller regulates the power flow between DG units and energy storage units to stabilize dc-link power. The suggested controller switches the energy storage unit's operating mode to charging mode in order to reduce the power on the dc-link. The suggested method determines when DGs and energy storage systems should operate in the presence of disruptions like voltage sag. The amount of energy that has to be stored is discovered through simulations for different voltage disruptions. Fig. 12, displays the active power that energy storage will absorb from the dc-link under various sag situations.

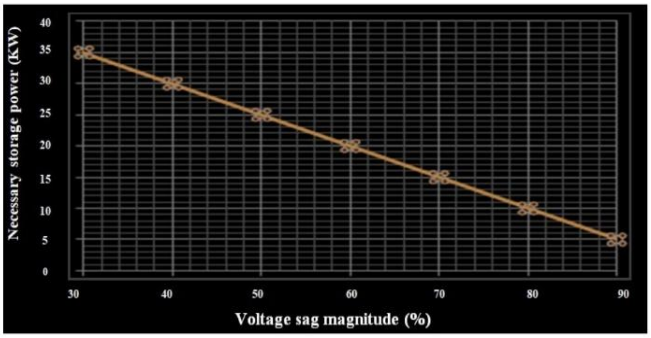

Fig. 12. Amount of necessary power to be stored during different percentage voltage sag magnitude.

4.3. Case 3: Voltage Regulation Ability During Unbalanced Conditions

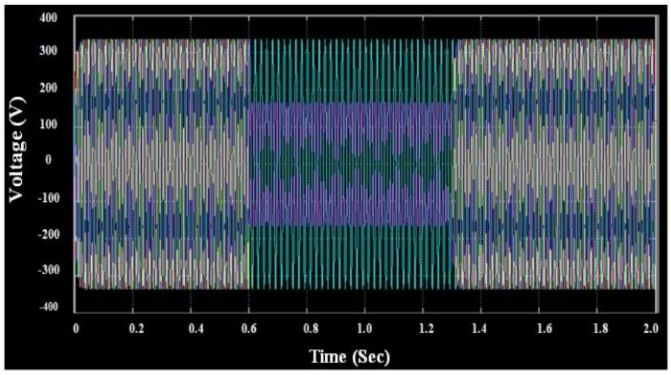

Fig. 13. Grid voltage during unbalance sag.

For evaluating the performance of voltage regulation under unbalanced grid conditions due to fault or sudden increase in load proposed PSO based fuzzy-AI tuned voltage controllers are tested. The sag of 60% magnitude is created by inducing a two-phase fault at grid side. Fig. 13, shows the grid voltage at the point of common coupling during unbalanced voltage sag. From the figure it is clear unbalance has been initiated for a certain time period, wherein there is a magnitude difference in the

phase grid voltages.

Due to unbalance in the system, the dual current controller injects positive and negative sequence current and voltages which will produce suitable PWM pulses for voltage source converter. Fig. 14 and Fig. 15 shows the current sequence components due to controller action under UC.

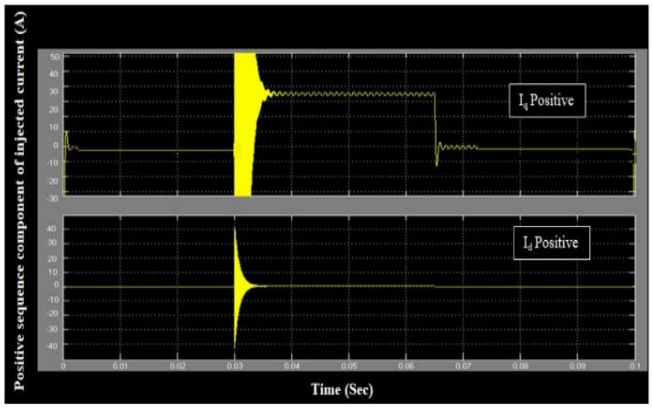

Fig. 14. Components of the injected current's positive sequence during imbalance.

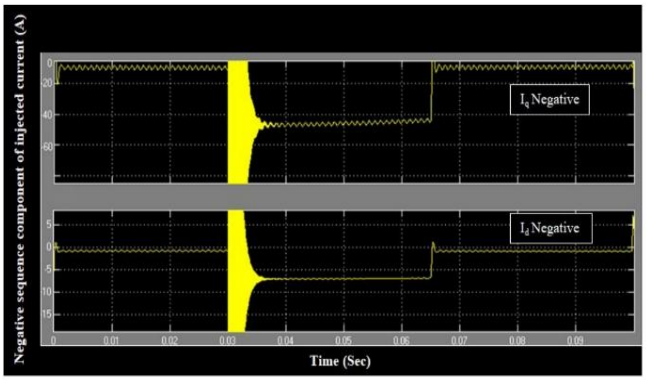

Fig. 15. Negative sequence components of injected current during unbalance.

The positive sequence components of the grid voltage are shown in Fig. 16, while the negative sequence components are shown in Fig. 17.

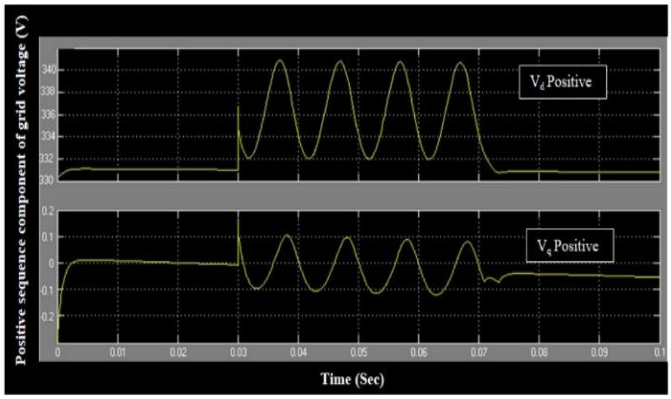

Fig. 16. Components of grid voltage in a positive sequence.

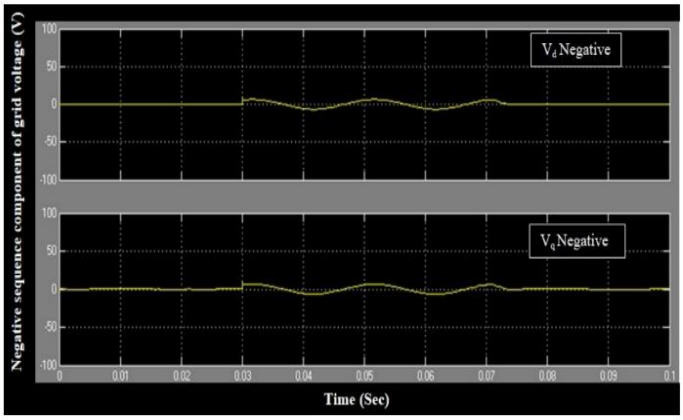

Fig. 17. Grid voltage's negative sequence components.

It is visible from the figures that only the positive sequence 'd' component of grid voltage is present and rest of the components vanish. It is because of the support of the interface inverter that responds in a faster way. The amount of reactive power for regulating the voltage is shown in Fig. 18. Because of this, the voltage is regulated during such disturbances. Fig. 19, shows the regulated voltage after grid voltage disturbances. Fig. 20, depicted as soft charging double boost MDC switching pulse schemes in 10ms. Fig. 21, proposed experimental results for capacitor voltage &current for soft charging MDC unit.

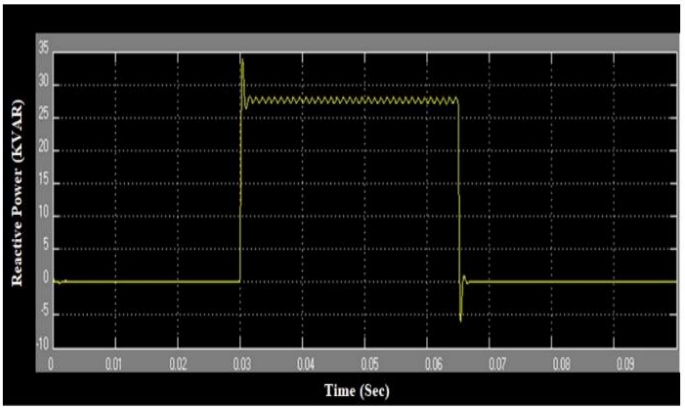

Fig. 18. Injected reactive power.

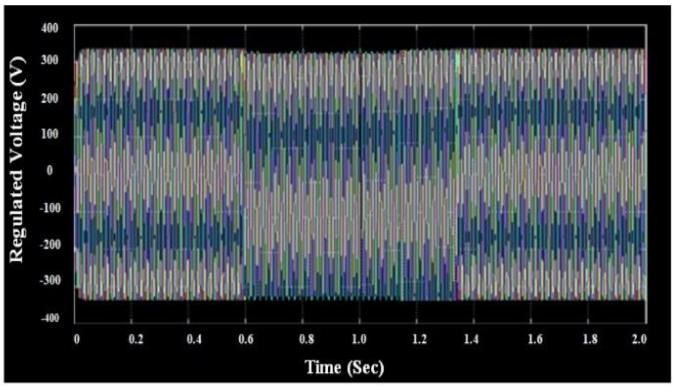

Fig. 19. Regulated voltages at point of common coupling.

Figure 22 proposed SSI inverter output with double boost MDC unit. Simulation results are compared with the previous literature [14]. It has already done experimental work in a slight UC made in between 0.2-0.4 sec, and the extreme unbalances during 0.4-0.6 sec. Hence, the unbalanced degree voltage compensation control was described as 0.25%. Here in the proposed work, an unbalance is created between 0.03 to 0.07 s, and the unbalanced voltage compensation is reported as 0.35%.

Table 3. Comparison of MDC Soft Charging Unbalanced phase voltage.

Author's Compare Existing Methods in Unbalanced phase voltage	Unbalanced % degree compensation
Ren et al., 2018 [31]	0.25
Bharath et al., 2019 [32]	2.5
Bimbhra and Garg 2014 [33]	0.30
Cougo et al., 2020 [34]	0.25
Linzen et al., 2002 [35]	0.35
Modified Soft Charging Boost Dual Controller (Proposed Method)	0.35

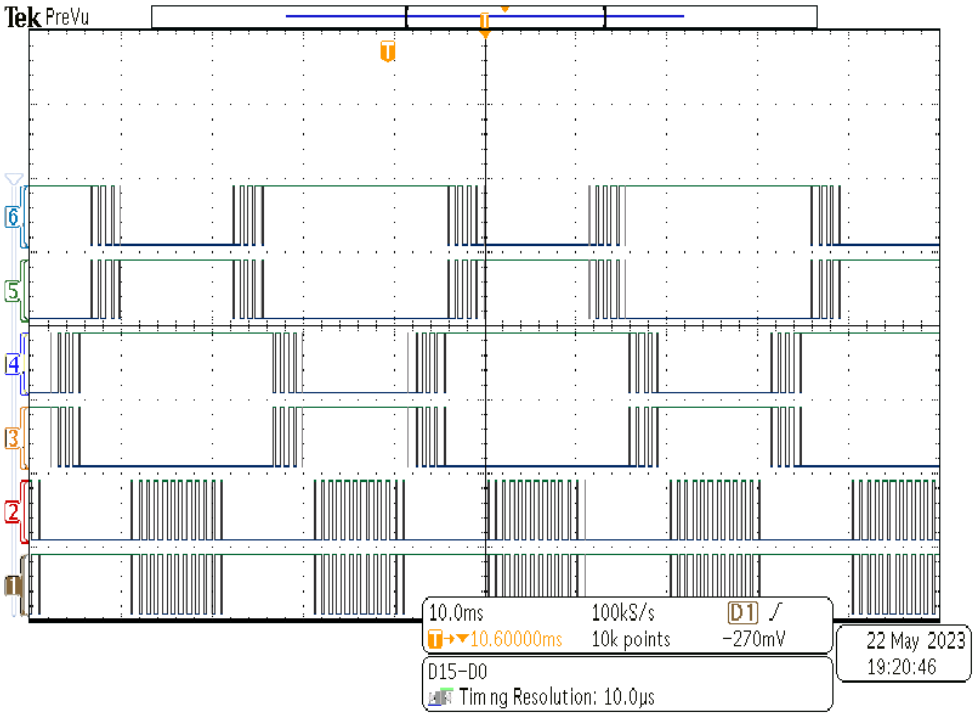

Fig. 20. Proposed Soft charging double boost MDC switching pulse.

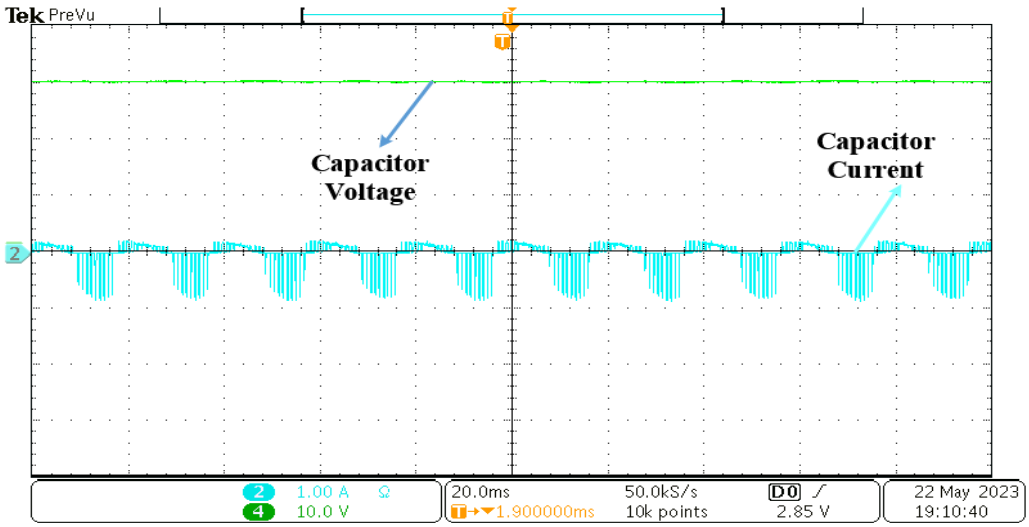

Fig. 21. Proposed experimental results (Capacitor Voltage & Current).

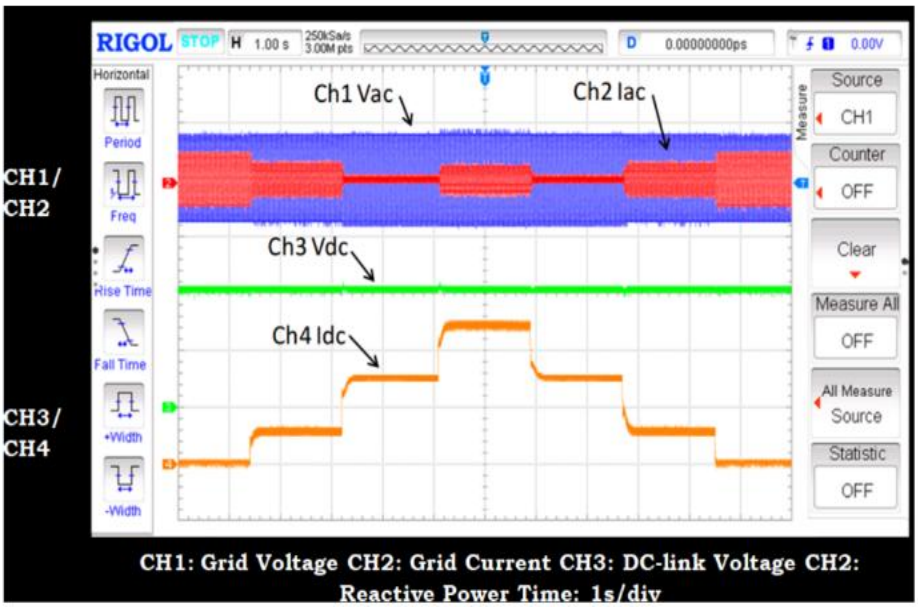

Fig. 22. Proposed SSI output in different channel.

The results from experiments clearly demonstrate that the SCDB-MDC can limit imbalance, correct for reactive power, and sustain voltage stability. By providing more voltage regulation, reduced current oscillations, and more rapid reaction times, it performs more effectively than traditional methods and ensures increased operational reliability during grid outages. In medium-voltage unbalanced grid networks, such measurements demonstrate the improvements over conventional methods and prove it to be effective.

5. Conclusion

A unique SSI inverter topology, employing switched double boost MDC generation has been proposed inside the paper. The AI fuzzy tuned approach of less switch counts based SSI inverter topology has been proposed, but traditional topology switches 9 switches or more. The gentle charging function within the proposed topology makes necessity of a low-price capacitor and its charging method. The present PWM technique has been used power to the switches. The switches are precipitated with fundamental switching; it makes minimize the switching loss. The designed inverter and its performance have been evaluated under the wide variety of dynamic situations such as trade of load, modulation indices, and output frequency exchange in MATLAB-Simulink platform. Oscillation inactive power due to voltage unbalance in three-phase system is suppressed using the proposed work Fuzzy-AI technique. Grid currents reach higher value during the distributing time. A modifying the current reference calculation in the proposed PSO based fuzzy-AI controller reached maximum iteration. A control strategy is developed such that DGs would be connected during disturbances and provides voltage support without affecting the converter. Voltage regulation capability and power transfer capability gets improved during voltage disturbances at the grid load side. More reactive power could not be injected for compensating additional voltage drop. This is the limitation and it depends on the capacity of the DG units and the grid. Therefore, mitigation of voltage sag is not possible, when the voltage drop is more than 90%.

Acknowledgements

The author would like to express his heartfelt gratitude to the supervisor for his guidance and unwavering support during this research for his guidance and support.

References

1. Salem A, Van Khang H, Robbersmyr KG, Norambuena M, Rodriguez J. Voltage source multilevel inverters with reduced device count: Topological review and novel comparative factors. IEEE transactions on power electronics. 2020 Jul 27;36(3):2720-47. https://doi.org/10.1109/TPEL.2020.3011908

2. Muisyo IN, Muriithi CM, Kamau SI. STATCOM Controller Tuning to Enhance LVRT Capability of Grid-Connected Wind Power Generating Plants. Journal of Electrical and Computer Engineering. 2022;2022(1):2873053.
3. Salama HS. *Applications of Energy Storage to Improve Performance of Utility Grids in Presence of Renewable Energies and Electric Vehicles* (Doctoral dissertation, Budapest University of Technology and Economics (Hungary)).
4. Kryltcov S, Makhovikov A, Korobitcyna M. Novel approach to collect and process power quality data in medium-voltage distribution grids. Symmetry. 2021 Mar 12;13(3):460. https://doi.org/10.3390/sym13030460
5. Salama HS, Vokony I. Voltage and Frequency Control of Balanced/Unbalanced Distribution System Using the SMES System in the Presence of Wind Energy. Electricity. 2021 Jun 1;2(2):205-24. https://doi.org/10.3390/electricity2020013
6. Kotb KM, Elmorshedy MF, Salama HS, Dán A. Enriching the stability of solar/wind DC microgrids using battery and superconducting magnetic energy storage based fuzzy logic control. Journal of Energy Storage. 2022 Jan 1;45:103751.
7. Alkhafaji AS, Trabelsi H. Survey a Superconducting Magnetic Energy Storage SMES with PV System to Enhance the Microgrid. In2022 19th International Multi-Conference on Systems, Signals & Devices (SSD) 2022 May 6 (pp. 1628-1637). IEEE. https://doi.org/10.1109/SSD54932.2022.9955824
8. Agajie TF, Fopah-Lele A, Ali A, Amoussou I, Khan B, Elsisi M, Nsanyuy WB, Mahela OP, Álvarez RM, Tanyi E. Integration of superconducting magnetic energy storage for fast-response storage in a hybrid solar PV-biogas with pumped-hydro energy storage power plant. Sustainability. 2023 Jul 7;15(13):10736.
9. Sarker K, Sarkar K, Sarker J, Bhowmik P, Chatterjee D, Goswami SK. Power quality investigation with multilevel inverter by photovoltaic-fed dynamic voltage restorer. International Journal of Modelling and Simulation. 2024 Mar 14:1-27. https://doi.org/10.1080/02286203.2024.2327647
10. Agajie TF, Fopah-Lele A, Amoussou I, Ali A, Khan B, Mahela OP, Nuvvula RS, Ngwashi DK, Soriano Flores E, Tanyi E. Techno-economic analysis and optimization of hybrid renewable energy system with energy storage under two operational modes. Sustainability. 2023 Jul 30;15(15):11735. https://doi.org/10.3390/su151511735
11. Taghvaie Gelehkolaee A. *Design, Modelling and Control of Grid Connected Solar Photovoltaic System with Solid-state Transformer* (Doctoral dissertation, Deakin University).
12. Zulu ML. *Power flow and faults analysis of a hybrid DC Microgrid: PV system and wind energy* (Doctoral dissertation).
13. Iweh CD, Gyamfi S, Tanyi E, Effah-Donyina E. Distributed generation and renewable energy integration into the grid: Prerequisites, push factors, practical options, issues and merits. Energies. 2021 Aug 29;14(17):5375. https://doi.org/10.3390/en14175375
14. Abdul Basit B, Nguyen AT, Ryu SW, Park H, Jung JW. A state-of-the-art comprehensive review of modern control techniques for grid-connected wind turbines and photovoltaic arrays distributed generation systems. IET Renewable Power Generation. 2022 Aug;16(11):2191-222. https://doi.org/10.1049/rpg2.12511
15. Yameen MZ, Lu Z, Rao MA, Mohammad A, Nasimullah, Younis W. Improvement of LVRT capability of grid-connected wind-based microgrid using a hybrid GOA-PSO-tuned STATCOM for adherence to grid standards. IET Renewable Power Generation. 2024 Nov;18(15):3218-38. https://doi.org/10.1049/rpg2.13036
16. Hasheminasab S, Alzayed M, Chaoui H. A Review of Control Techniques for Inverter-Based Distributed Energy Resources Applications. Energies. 2024 Jun 14;17(12):2940. https://doi.org/10.3390/en17122940
17. Hattabi I, Kheldoun A, Bradai R, Khettab S, Sabo A, Belkhier Y, Khosravi N, Oubelaid A. Enhanced power system stabilizer tuning using marine predator algorithm with comparative analysis and real time validation. Scientific Reports. 2024 Nov 22;14(1):28971. https://doi.org/10.1038/s41598-024-80154-2
18. El Sayed NG, Yousef AM, El-Saady G, Alanazi MD, Ziedan HA, Abdelsattar M. Artificial intelligent fuzzy control and LAPO algorithm for enhancement LVRT and power quality of grid connected PV/wind hybrid systems. Scientific Reports. 2024 Dec 16;14(1):1-42. https://doi.org/10.1038/s41598-024-78384-5
19. Yegon P, Singh M. Optimization of battery/ultra-capacitor hybrid energy storage system for frequency response support in low-inertia microgrid. IET Power Electronics. 2024. https://doi.org/10.1049/pel2.12723
20. Mondal S, Biswas SP, Islam MR, Muyeen SM. A five-level switched-capacitor based transformerless inverter with boosting capability for grid-tied PV applications. IEEE Access. 2023 Feb 3;11:12426-43. https://doi.org/10.1109/ACCESS.2023.3241927

21. Ravi T, Sathish Kumar K. Analysis, monitoring, and mitigation of power quality disturbances in a distributed generation system. Frontiers in Energy Research. 2022 Nov 7;10:989474.
22. Iweh CD, Gyamfi S, Tanyi E, Effah-Donyina E. Distributed generation and renewable energy integration into the grid: Prerequisites, push factors, practical options, issues and merits. Energies. 2021 Aug 29;14(17):5375. https://doi.org/10.3390/en14175375
23. Alharbi M. Control Approach of Grid-Connected PV Inverter under Unbalanced Grid Conditions. Processes. 2024 Jan 18;12(1):212. https://doi.org/10.3390/pr12010212
24. Alathamneh M, Ghanayem H, Yang X, Nelms RM. Three-Phase Grid-Connected Inverter Power Control under Unbalanced Grid Conditions Using a Proportional-Resonant Control Method. Energies. 2022 Sep 26;15(19):7051. https://doi.org/10.3390/en15197051
25. Joshi J, Jately V, Kala P, Sharma A, Lim WH, Azzopardi B. Control strategy for current limitation and maximum capacity utilization of grid connected PV inverter under unbalanced grid conditions. Scientific Reports. 2024 May 2;14(1):10118. https://doi.org/10.1038/s41598-024-60244-x
26. Nikolaev N, Dimitrov K, Rangelov Y. A comprehensive review of small-signal stability and power oscillation damping through photovoltaic inverters. Energies. 2021 Nov 5;14(21):7372. https://doi.org/10.3390/en14217372
27. Tiwari A, Agarwal R. Soft charging and fewer switches based single-source double-boost multilevel DC-AC converter for low/medium voltage applications. International Journal of Circuit Theory and Applications. 2024. https://doi.org/10.1002/cta.4176
28. Hata K, Tanaka S, Ashikaga T, Rikiishi Y. Always-Dual-Path Hybrid DC-DC Converter with Soft Charging for High Efficiency with Reduced Passive Components. In2024 IEEE Applied Power Electronics Conference and Exposition (APEC) 2024 Feb 25 (pp. 1371-1376). IEEE. https://doi.org/10.1109/APEC48139.2024.10509498
29. Abbasi M, Abbasi E, Li L, Tousi B. Design and analysis of a high-gain step-up/down modular DC–DC converter with continuous input current and decreased voltage stress on power switches and switched-capacitors. Sustainability. 2021 May 7;13(9):5243. https://doi.org/10.3390/su13095243
30. Anand V, Singh V, Ali JS. Dual boost five-level switched-capacitor inverter with common ground. IEEE Transactions on Circuits and Systems II: Express Briefs. 2022 Apr 20;70(2):556-60. https://doi.org/10.1109/TCSII.2022.3169009
31. Ren B, Sun X, Chen S, Liu H. A compensation control scheme of voltage unbalance using a combined three-phase inverter in an islanded microgrid. Energies. 2018 Sep 18;11(9):2486. https://doi.org/10.3390/en11092486
32. Bharath GV, Hota A, Agarwal V. A new family of 1-φ five-level transformerless inverters for solar PV applications. IEEE Transactions on Industry Applications. 2019 Sep 23;56(1):561-9. https://doi.org/10.1109/TIA.2019.2943125
33. Bimbhra PS, Garg GC. Electrical machines-I. Khanna Publishing House; 2014. https://www.scribd.com/doc/281602320/Power-Electronics-Dr-P-S-BIMBHRA-1
34. Cougo B, Morais LM, Segond G, Riva R, Tran Duc H. Influence of PWM methods on semiconductor losses and thermal cycling of 15-kVA three-phase SiC inverter for aircraft applications. Electronics. 2020 Apr 7;9(4):620. https://doi.org/10.3390/electronics9040620
35. Linzen D, De Doncker RW. Simulation of power losses with MATLAB/Simulink using advanced power device models. In2002 IEEE Workshop on Computers in Power Electronics, 2002. Proceedings. 2002 Jun 3 (pp. 71-75). IEEE. https://doi.org/10.1109/CIPE.2002.1196718